SAKARYA UNIVERSITY JOURNAL OF COMPUTER AND INFORMATION SCIENCES
http://saucis.sakarya.edu.tr/
e-ISSN: 2636-8129
Publisher: Sakarya University
Vol. 8, No. 3, 441-456, 2025
DOI: 10.35377/saucis...1650707
SAUCIS
SAKARYA UNIVERSITY
RESEARCH ARTICLE

NOMA-Integrated Interleave-Division Multiple Access: A Beyond 5G Perspective

Shivani Dixit[1], Özkan Canay[2,*], Varun Shukla[3], Manoj Kumar Misra[4]

[1]Pranveer Singh Institute of Tech., Dept. of Electronics & Communication, Kanpur, India,
[2]Sakarya University, Dept. of Information Systems and Technologies, Sakarya, Türkiye, ror.org/04ttnw109
[3]Allenhouse Institute of Technology, Dept. of Electronics & Communication, Kanpur, India,
[4]Allenhouse Institute of Technology, Dept. of Computer Science, Kanpur, India,

Corresponding author:
Özkan Canay
Sakarya University
Dept. of Information Systems and Tech.
Sakarya, Türkiye
canay@sakarya.edu.tr

Article History:
Received: 05.03.2025
Revised: 06.07.2025
Accepted: 09.08.2025
Published Online: 26.09.2025

ABSTRACT
Efficient multiple access is vital for spectrum-constrained, user-dense IoT networks. This study joins interleave-division multiple access (IDMA) with power-domain non-orthogonal multiple access (NOMA) and employs ordered successive-interference-cancellation multi-user detection (SIC-MUD). Unequal power allocation and orthogonal interleavers let all users share one spreading code while keeping chip-level complexity low. Simulations of a five-user uplink and a thirty-two-user downlink show that the worst user attains a bit-error rate of 1.4×10^{-3} at 10 dB, needing ≈ 3 dB less SNR than equal-power IDMA; flat Rayleigh fading raises the curve by only ≈ 2 dB. A software detector processes 2048-bit frames in ≈ 0.03 s on a standard desktop, and cycle estimates predict under 5 ms latency on a 32-100 MHz FPGA. Random interleaving gives the lowest error rate, while master-random and tree-based patterns lose < 0.3 dB yet cut memory sharply. Ordered SIC-MUD NOMA-IDMA thus offers concrete performance gains and real-time feasibility for dense 6G and massive-IoT deployments.

Keywords: Non-Orthogonal Multiple Access (NOMA), Interleave-Division Multiple Access (IDMA), Successive Interference Cancellation (SIC), Multi-User Detection (MUD), Spectrum Efficiency

1. Introduction

The rapid advancement of wireless communication technologies has accelerated the transition from 5G to next-generation 6G networks, driven by the demand for higher data rates, lower latency, and improved scalability [1,2,25]. With the rapid expansion of IoT applications, conventional orthogonal multiple access (OMA) techniques such as TDMA, FDMA, and CDMA struggle to accommodate the growing number of connected devices because of their rigid resource allocation constraints [3-6]. To meet these increasing demands, next-generation wireless networks aim to enhance spectrum efficiency and improve multiple access strategies while maintaining ultra-reliable low-latency communication (URLLC) [4,5].

OMA techniques rely on strict orthogonal resource allocation, ensuring non-overlapping spectrum sharing among users. While this approach simplifies receiver design and reduces interference, it inherently limits the number of simultaneous connections and spectral efficiency [7]. Additionally, random channel impairments disrupt the orthogonality of OMA systems, increasing decoding complexity and reducing system performance in high-user-density environments [8].

To overcome these challenges, non-orthogonal multiple access (NOMA) has emerged as a more scalable solution for future wireless networks [9,10]. Unlike OMA, which strictly separates resources among users, NOMA enables multiple users to share the same frequency, time, or code resources. This shared-resource access is realized either through power-domain NOMA, which assigns different power levels to users, or code-domain NOMA, which separates users via unique coding schemes [9,10]. The 3rd Generation Partnership Project (3GPP) has classified NOMA into these two primary strategies [11]. Power-domain NOMA assigns different power levels to users, enabling successive interference cancellation (SIC) at the receiver to separate signals based on power differences [12]. Meanwhile, code-domain NOMA distinguishes users through specific spreading sequences or interleaving patterns [13].

Interleave-division multiple access (IDMA), a form of code-domain NOMA, has attracted attention due to its low-complexity multi-user detection (MUD) capability based on user-specific interleaving. By assigning unique interleavers to users, IDMA reduces multi-user interference and enables efficient joint detection [12]. However, conventional IDMA schemes typically assume equal power allocation among users, which may not be optimal in high-user-density scenarios [14]. Recent research

Cite as: S. Dixit, Ö. Canay, V. Shukla and M. Kumar Misra. (2025). NOMA-integrated interleave-division multiple access: A beyond 5G perspective. *Sakarya University Journal of Computer and Information Sciences*. vol. 8, no. 3, pp. 441-456, 2025 doi: 10.35377/saucis...1650707

has explored the integration of power-domain NOMA with IDMA (NOMA-IDMA) to enhance spectral efficiency and user separation [15,16]. In this hybrid system, unequal power levels are assigned to users, improving the effectiveness of SIC-based detection while leveraging the inherent benefits of IDMA's interleaving process.

Despite the advantages of NOMA-IDMA, a central challenge lies in decoding user signals efficiently, which depends on the implementation strategy of successive interference cancellation with multi-user detection (SIC-MUD) [17,18]. Prior studies have primarily focused on unordered SIC-MUD, where users are decoded in an arbitrary order [19,20]. While unordered SIC simplifies implementation, it suffers from higher error propagation, especially in high-user-density environments [21]. Ordered SIC-MUD, where users are decoded sequentially based on their power levels, has been proposed to mitigate this issue and enhance decoding reliability [22,23]. However, while ordered SIC-MUD has been explored in various NOMA applications, its role in improving error resilience and decoding performance in NOMA-IDMA systems, particularly under dense-user conditions, remains insufficiently studied.

Recent studies have increasingly investigated the integration of Non-Orthogonal Multiple Access (NOMA) and Interleave-Division Multiple Access (IDMA) to address the growing demands for efficiency and scalability in next-generation wireless systems. These studies cover various topics, including bit error rate (BER) performance, power allocation strategies, and multi-user detection techniques. Table 1 presents a selection of recent contributions directly related to this work's objectives and evaluation criteria.

Table 1. Recent Studies on NOMA-IDMA Systems and Related Multi-Access Techniques

Key contribution	**Method**	**Findings**	**Author, Year [Ref.]**
First detailed performance analysis of active-passive hybrid RIS + NOMA	Monte Carlo link-level simulation with a realistic RIS model	The hybrid RIS improved overall throughput and spectral efficiency and achieved lower BER than passive RIS.	Kumaradasa et al., 2025 [28]
Joint offloading & resource-allocation framework for NOMA-VEC	Decision-loop successive optimization / Convex optimization techniques	Reduced end-to-end delay and improved energy efficiency in vehicular networks.	Dong et al., 2025 [29]
New precoder design based on constructive interference for IRS-NOMA	Convex phase/power optimization	Achieved higher aggregate spectral efficiency and potential power savings through optimized precoding.	Cui et al., 2025 [30]
Convergence analysis for OFDMA-IDMA uplink blend under 802.11ax	MATLAB PHY demo / Theoretical analysis + BER measurement	Demonstrated the benefits of the OFDMA-IDMA combination in 802.11ax, potentially supporting more users.	Ta et al., 2024 [31]
Scalability tests of resource-unit mapping for OFDMA-IDMA	NS-3 simulation + real hardware test-bed	Showed improved total data rate and stable BER performance for massive uplink scenarios.	Ta et al., 2024 [32]
Comprehensive survey of NOMA in satellite-air-ground integration	Review article/survey analysis	Highlighted NOMA's significant spectrum efficiency gains in non-terrestrial network integration.	Ding et al., 2024 [33]
Covert-transmission framework using RIS-NOMA for Integrated Sensing and Communication (ISAC)	Two-stage constrained optimization	Enhanced secret data rate for covert communication in ISAC systems by leveraging RIS-NOMA.	Yu et al., 2024 [34]
New TD-NOMA scheme incorporating transmit diversity for low latency	2 × 2 MIMO hardware test / Performance analysis	Improved low-latency communication and reduced error rates by combining NOMA with transmit diversity.	Moriyama et al., 2023 [35]
Queue-aware resource allocation combining STAR-RIS and NOMA	Lyapunov-based online algorithm	Achieved higher stable average rates by optimizing resource allocation considering queue status.	Chen et al., 2023 [36]
Energy-delay trade-off analysis in RIS-NOMA MEC networks in finite blocklength	Mixed-integer programming + successive refinement	Demonstrated energy savings and guaranteed URLLC performance in RIS-NOMA MEC networks.	Zhao et al., 2023 [37]
Analytical framework for MC-Q-NOMA under α-μ fading channel	Closed-form BER & capacity expressions	Provided analytical insights into SNR gain and capacity improvements for MC-Q-NOMA in specific fading.	Cui et al., 2023 [38]
Impact of NOMA on Age of Information (AoI) in grant-free transmission models	Queue-theory analysis + simulation	Showed that NOMA (grant-free) can reduce AoI compared to traditional methods like TDMA.	Wu et al., 2023 [39]

This research investigates the effect of ordered SIC-MUD on bit error rate (BER) performance in NOMA-IDMA systems, focusing on uplink and downlink transmissions. The primary question of the research is whether ordered SIC-MUD significantly enhances system performance compared to unordered SIC-MUD, particularly in dense-user scenarios. To systematically address this question, the study aims to:

1. Develop and analyze an ordered SIC-MUD framework for NOMA-IDMA systems.
2. Compare the BER performance of ordered and unordered SIC-MUD in various user-density conditions.
3. Evaluate the potential of ordered SIC-MUD to enhance decoding reliability in practical deployments.

The rest of this paper is organized as follows. Section 2 presents the system model, including transmitter and receiver structures with SIC-MUD. Section 3 outlines the methodology, covering simulation settings, performance metrics, and implementation details. Section 4 reports the simulation results, such as factor analysis, BER trends under different channels, runtime analysis, and interleaver comparisons. Section 5 discusses these findings in light of related work, and Section 6 concludes with a summary and future directions.

2. IDMA and NOMA-IDMA System Model

Power-domain non-orthogonal multiple access (NOMA) and interleave-division multiple access (IDMA) are complementary schemes designed to improve spectral efficiency in multi-user wireless networks. In conventional IDMA, users are separated by distinct orthogonal interleavers, enabling simultaneous access over the same time-frequency resources with equal power levels [12]. When unequal power allocation is incorporated, the resulting structure is called NOMA-IDMA. This approach combines power-domain multiplexing with chip-level user separation, improving interference management and overall throughput.

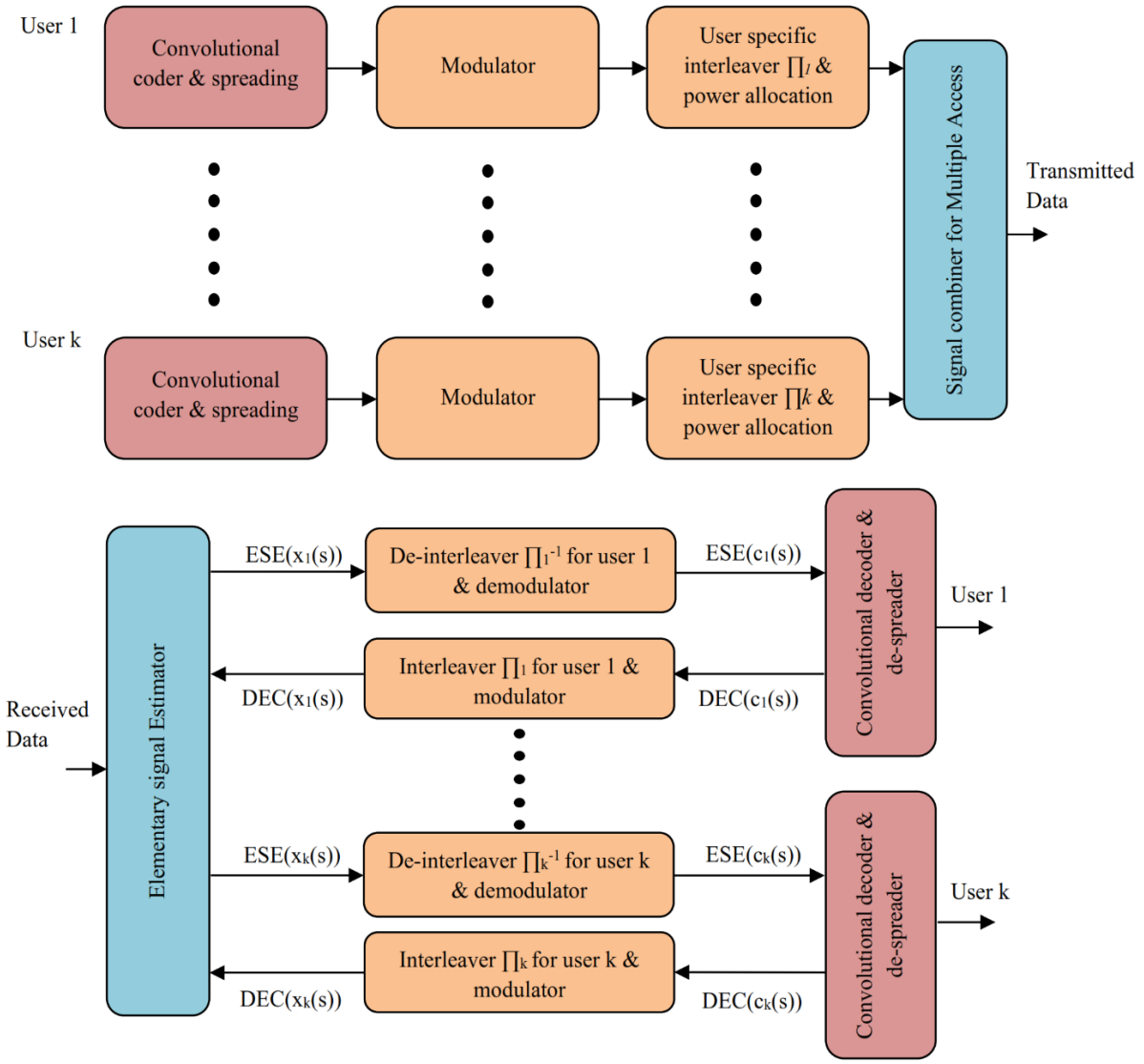

Figure 1. Transmitter and Receiver Structure of NOMA-IDMA and IDMA Scheme

The 3rd Generation Partnership Project (3GPP) classifies NOMA techniques into two broad categories: power-domain NOMA [9] and code-domain NOMA [10]. In the power-domain variant, multiple users share the same spectrum by being assigned different power levels. These signals are decoded at the receiver using successive interference cancellation with multi-user detection (SIC-MUD) [9, 11], where each decoded signal is subtracted from the received mixture to reduce interference for the remaining users. Further gains in spectral efficiency can be achieved by combining NOMA with multiple-input multiple-output (MIMO) systems [11]. Cooperative NOMA is another variation in which a strong user assists weaker users by relaying their data, improving link reliability under challenging channel conditions. The complete transmitter and receiver structure of the NOMA-IDMA system, including the user-specific processing stages and multi-user detection at the receiver, is shown in Figure 1.

2.1 Transmitter Structure

In the NOMA-IDMA scheme with *K* users, each user first encodes its information bits using a rate-1/2 convolutional code. The resulting coded bits are then BPSK-modulated into a bipolar chip sequence, $x_k(s) \in \{+1, -1\}$ for $s = 1, \ldots, S$, where S is the chip length. This sequence is spread using a user-specific spreading code and passed through an orthogonal interleaver Π_k, selected from a set of *K* orthogonal interleavers [12, 15-19].

After interleaving, each chip $x_k(s)$ is multiplied by the amplitude coefficient $\sqrt{\beta_k}$. Here, β_k ($0 < \beta_k < 1, \sum_{k=1}^{K} \beta_k = 1$) denotes the fraction of the total transmit power allocated to user *k*; thus, user *k* transmits with power $\beta_k P_S$. Noise variance is normalised to unity, so P_S represents both the total transmit power and the total signal-to-noise power ratio. In the equal-power (IDMA) case, $\beta_k = 1$, whereas in NOMA-IDMA the β_k values are chosen optimally to support successive interference cancellation. Then, the weighted signals from all K users are summed up and transmitted over an AWGN channel.

2.2 Receiver Structure

In a NOMA-IDMA system, the receiver plays a crucial role in decoding multiple user signals efficiently while mitigating interference. The use of SIC-MUD enables sequential cancellation of user interference, which improves detection accuracy in high-user-density scenarios. The user ordering strategy further enhances the effectiveness of SIC-MUD by prioritizing users based on their power levels. An efficient user ordering and power allocation scheme for successive interference cancellation in NOMA was introduced by Shin et al. [24], which can be adapted to power-domain NOMA-IDMA systems.

The incoming signal at the receiver is a composite of multiple users' transmissions, subjected to channel fading and additive white Gaussian noise (AWGN). The receiver must extract and decode each user's signal while maintaining computational efficiency. As shown in Fig. 1, the received combined signal from all the users can be represented as follows:

$$r(s) = \sum_{k=1}^{K} \sqrt{\beta_k P_S} h_k x_k(s) + w(s), \quad s = 1, \ldots, S \tag{1}$$

Here β_k denotes the power-allocation coefficient for user *k* ($\beta_k = 1$ in the equal-power IDMA case), h_k its channel gain, P_S is the total signal-to-noise power ratio, $x_k(s) \in \{+1, -1\}$ is the BPSK chip at time index $s = 1, \ldots, S$, and $w(s) \sim \mathcal{N}(0, 1)$ is the AWGN sample, with noise variance normalised to unity.

NOMA-IDMA receiver decodes the data of multiple users with the SIC-MUD algorithm. The concept of NOMA-aided massive MIMO systems with SIC-MUD implementation has been explored by Kusaladharma et al. [26], where the performance of NOMA is significantly improved in cell-free massive MIMO scenarios. When equal power is used, the MUD operation in NOMA-IDMA follows the same structure as conventional IDMA[12]. However, in SIC-MUD implementation, users are ordered according to the power levels assigned at the transmitter. The traditional procedure of MUD then follows, where interference is subtracted successively for each user.

For implementing MUD at the receiver end, the Elementary Signal Estimator (ESE) estimates the interleaved chip-level signal for each user, assuming perfect channel estimation at the receiver [12]. The signal expression mentioned in Eq. (1) for a specific user (*k*) can also be written as Eq. (2).

$$r(s) = \sqrt{\beta_k P_S} h_k x_k(s) + \xi_k(s) \tag{2}$$

This representation indicates $\xi_k(s)$ as multiple access interference from other users and $\sqrt{\beta_k P_S} h_k x_k(s)$ as the intended user signal. The multiple access interference can be written as Eq. (3).

$$\xi_k(s) \equiv r(s) - \sqrt{\beta_k P_S} h_k x_k(s) = \sum_{i \neq k} \sqrt{\beta_i P_S} h_i x_i(s) + w(s) \tag{3}$$

Assuming $\xi_k(s)$ is a Gaussian random variable with mean $\mathrm{E}\{\xi_k(s)\}$ and variance $\mathrm{Var}\{\xi_k(s)\}$, the log-likelihood ratio (LLR)

at the output of the ESE for user k is given by Eq. (4).

$$e_{ESE}(x_k(s)) = \frac{2\sqrt{\beta_k P_S}\, h_k\,[\, r(s) - E\{\xi_k(s)\}\,]}{Var\{\xi_k(s)\}} \tag{4}$$

These LLR values are passed through an a-posteriori probability (APP) decoder after de-interleaving, demodulation, and despreading. The decoder outputs are then fed back into the ESE, repeating the same processing stages as the transmitter. This iterative exchange of information continues for a predefined number of iterations to minimize the bit error rate (BER) [12].

To further improve BER performance, especially under varying power levels, the average signal-to-interference-plus-noise ratio (SINR) at the ESE output after the l^{th} iteration is mapped to a decoder output variance $f(SINR_k^{(l)})$. For an additive white Gaussian noise (AWGN) channel and L total iterations, the SINR can be recursively approximated as Eq. (5) [13]:

$$SINR_k^{(l+1)} = \frac{\beta_k P_S |h_k|^2}{\sum_{i \neq k} \beta_i P_S |h_i|^2 f_i\left(SINR_i^{(l)}\right) + 1}, \qquad l = 0, \ldots, L-1 \tag{5}$$

Here $f_i(\cdot)$ maps SINR to decoder extrinsic variance. For small K, we exhaustively search over $\{\beta_k\}$; for large K, we use the algorithm in [13], assuming $SINR_k^{(l)} \geq \alpha$ for all k.

SIC-MUD is a fundamental technique in power-domain NOMA and also forms the basis of the receiver design in NOMA-IDMA systems [9, 11]. In this structure, the receiver decodes multiple user signals using successive interference cancellation combined with multi-user detection. The decoding process can follow two diverse approaches: unordered SIC, where users are processed in a fixed sequence regardless of power levels, and ordered SIC, which prioritizes decoding based on power allocation or channel conditions. The choice of ordering strategy significantly affects system performance, particularly in dense-user scenarios. NOMA-integrated IDMA adopts SIC-MUD to exploit these strategies and improve decoding reliability. A summary of the key differences between unordered and ordered SIC approaches is presented in Table 2.

Table 2. Comparison of Ordered and Unordered NOMA-IDMA Decoding

Feature	Unordered NOMA-IDMA	Ordered NOMA-IDMA
Decoding Process	Each user decodes its signal independently without a specific order and subtracts it from the combined signal.	The user with the highest received power is decoded first, and its signal is subtracted from the combined signal.
SIC Procedure	Each user's signal is decoded and removed successively, but the order is not predefined.	Each user's signal is decoded in a predefined order, with stronger users decoded after weaker ones.
Error Propagation	A succeeding user's decoding probability is never better than the preceding.	A succeeding user might still be decoded correctly even if the preceding user's decoding fails.
Performance & Complexity	Lower computational complexity but higher risk of error propagation.	Improved performance but with additional computational complexity.

Ordered SIC offers greater decoding reliability in exchange for increased computational load, making it a key element in optimizing NOMA-IDMA performance. While unordered decoding simplifies implementation, it is more prone to error propagation. In contrast, ordered SIC-MUD prioritizes weaker users and improves overall interference management, especially in dense access scenarios.

2.3 SIC-MUD Implementation in NOMA-IDMA Receiver

In NOMA-IDMA systems with unequal power allocation, the receiver employs successive interference cancellation (SIC) combined with multi-user detection (MUD). Depending on the prioritization of users during decoding, the implementation can follow an unordered or an ordered manner. It is subtracted from the combined received signal to reduce interference for the remaining users and improve overall detection accuracy.

In unordered SIC-MUD, users are decoded in a fixed order, regardless of their power levels. This approach simplifies implementation but is more susceptible to error propagation. If a stronger user's signal is decoded early and incorrectly, the residual interference can compromise the decoding of subsequent users. In contrast, ordered SIC-MUD prioritizes users for decoding according to their received power levels. In the uplink, decoding typically begins with users assigned higher power, while in the downlink, it starts with users experiencing weaker channel gains. This ordering mitigates error propagation and improves robustness, especially in high-user-density scenarios. Due to these advantages, the ordered SIC-MUD strategy is adopted for both uplink and downlink configurations.

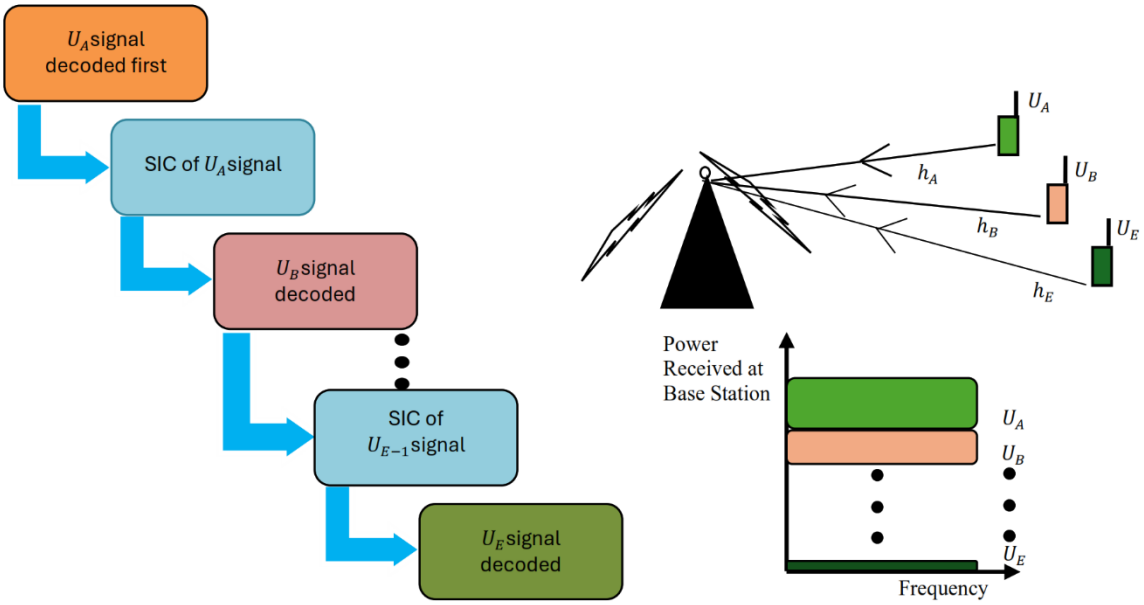

Figure 2. Uplink SIC-MUD Decoding at Base Station

In the uplink, the base station receives the superposed signals from multiple users. As illustrated in Figure 2, decoding begins with the user having the highest received power. Once this signal is removed, the following strongest user is decoded, and the process continues. This successive cancellation reduces interference at each stage and improves decoding success for weaker users. A study by Ding [20] has shown that NOMA can outperform OMA with optimized power allocation, which supports the following analysis.

For five users U_A through U_E, transmitting signals S_A to S_E, the received composite signal at the base station is:

$$Y_{BS} = h_A S_A \sqrt{\beta_A P_S} + h_B S_B \sqrt{\beta_B P_S} + \ldots + h_E S_E \sqrt{\beta_E P_S} + n_{\mathrm{BS}} \tag{6}$$

Here, h_k is the channel gain for user $\mathrm{U_k}$, β_k is the fraction of total transmit power P_S assigned to user k, and n_{BS} is the additive white Gaussian noise sample. The total power constraint requires that $\sum_{k=A}^{E} \beta_k = 1$.

Assuming descending channel gains such that $|h_A|^2 > |h_B|^2 > \cdots > |h_E|^2$, the signal-to-interference-plus-noise ratio (SINR) for decoding S_A at the base station becomes:

$$\mathrm{SINR}_{\mathrm{BS}}^{S_A} = \frac{|h_A|^2 \beta_A P_S}{1 + \sum_{i=B}^{E} |h_i|^2 \beta_i P_S} \tag{7}$$

Once S_A is decoded and subtracted, the SINR for decoding S_B improves accordingly:

$$\mathrm{SINR}_{\mathrm{BS}}^{S_B} = \frac{|h_B|^2 \beta_B P_S}{1 + \sum_{i=C}^{E} |h_i|^2 \beta_i P_S} \tag{8}$$

This cancellation process continues until the weakest user U_E is decoded, by which point all interfering signals from stronger users have been removed. This way, users with low power allocations can still achieve reliable decoding.

A similar approach applies in the downlink. In this case, each user receives the same superposed signal, and decoding begins with the user having the weakest channel. As illustrated in Figure 3, user U_A, having the smallest $|h_A|^2$, is allocated more transmit power to ensure decodability. Its signal is then removed from the received waveform, enabling U_B to decode with reduced interference.

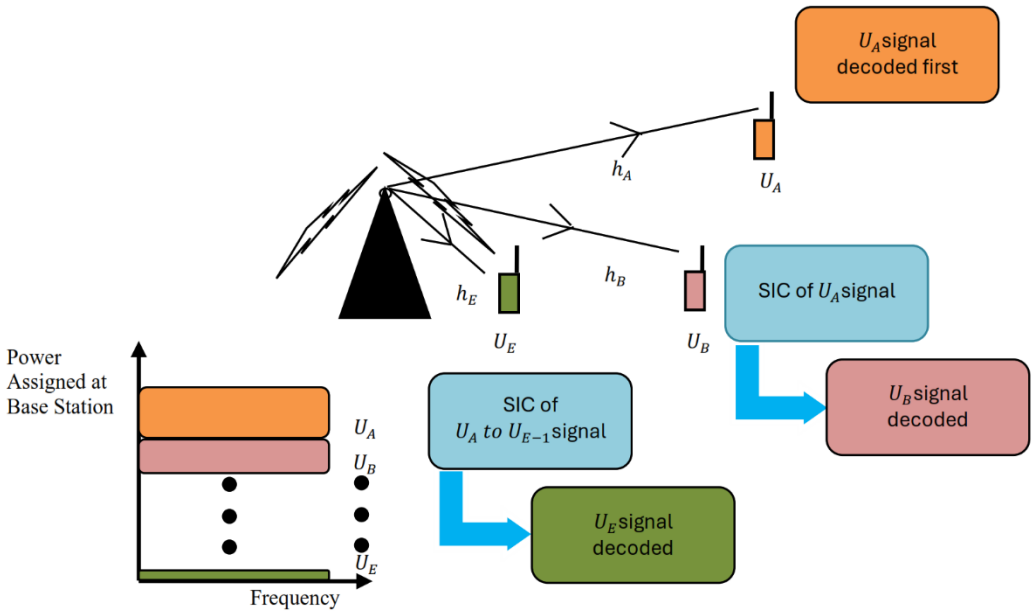

Figure 3. Downlink SIC-MUD Decoding at User Station

The received signal at user U_k is given by:

$$Y_k = \sum_{i=A}^{E} h_k S_i \sqrt{\beta_i P_S} + n_k \tag{9}$$

Here, S_i is the transmitted signal from user U_i, h_k is the path gain for user U_k, and n_k denotes the additive white Gaussian noise at user U_k. Assuming ascending channel gains across users, the SINR improves with each successive cancellation step. This structure allows even the lowest-power user to decode its message reliably, validating the use of ordered NOMA-IDMA for high-density communication scenarios.

3. Methodology

A structured methodology is adopted to evaluate the proposed NOMA-IDMA system with successive interference cancellation (SIC-MUD), encompassing detailed simulation settings, system parameters, and performance evaluation criteria. The analysis systematically compares the performance of NOMA-IDMA and conventional IDMA, emphasizing bit error rate (BER) performance under different configurations. Various interleaving techniques and power allocation strategies are incorporated into simulations, ensuring a fair and comprehensive assessment of their impact on system performance across multiple user densities.

3.1 Simulation Environment and Channel Model

The simulations were conducted using a MATLAB-based framework that models a NOMA-IDMA wireless communication system. Uplink and downlink transmissions were evaluated under an additive white Gaussian noise (AWGN) channel to measure the impact of power-allocation and interleaving schemes. The receiver is assumed to have perfect channel-state information (CSI), allowing accurate power-based user ordering in SIC-MUD decoding while avoiding errors due to channel estimation. Baseline runs use a standard AWGN model; additional tests cover a flat Rayleigh fading channel (see Subsection 4.2) to verify detector robustness under multipath.

3.2 System Model and Parameters

The multi-user transmitter consists of *K* independent sources. Each user first applies rate-1/2 convolutional encoding to its binary payload, followed by BPSK modulation. The modulated symbols are superimposed in the power domain and conveyed over an AWGN channel for baseline trials governed by Eq. (1); tests that include flat Rayleigh fading are described later in Subsection 3.4. Before transmission, every user sequence passes through an interleaver to reduce cross-correlation among spreading sequences and to ease multi-user detection (MUD) at the receiver.

Three interleaver designs are considered to examine the principal trade-offs among BER performance, memory footprint, and computational load:

- *Random interleaver* maximizes statistical independence between users but requires a large, unique look-up table.

- *Master-random interleaver* derives each user's pattern from a single master sequence, preserving near-random separation while significantly reducing storage.
- *Tree-based interleaver* generates deterministic, hierarchically related patterns that minimize on-chip memory and control logic, making it attractive for large hardware deployments.

Implementation details for these patterns are presented in Subsection 3.4, and their impact on system performance is quantified in Section 4. In these evaluations, the receiver adopts an ordered successive-interference-cancellation MUD (SIC-MUD), assuming perfect channel-state information (CSI) so users can be sorted by received power without estimation error. The decoding procedure is as follows:

1. Decode the strongest power user.
2. Subtract its reconstructed waveform from the composite signal.
3. Repeat for each remaining user until all K streams are recovered.

This iterative strategy reduces interference at each step.

3.3 Performance Evaluation Metrics

The system performance was evaluated based on bit error rate (BER) performance across different user densities and power allocation schemes. BER was chosen as the primary metric since it directly reflects the reliability of the multi-user detection process in NOMA-IDMA and conventional IDMA systems.

Simulations were conducted over an SNR range of 5 dB to 25 dB, and BER curves were plotted from 10^{-1} down to 10^{-5} to cover the reliability span typical of wireless links. Each run varies the interleaver type, SIC-MUD iteration count (1 to 5), and channel model (AWGN or flat Rayleigh) to isolate their individual effects on BER. Average per-frame CPU runtime was also logged to gauge real-time feasibility; these timing results are reported later in Subsection 4.3.

Simulations were run under two user configurations to evaluate the BER performance of the proposed NOMA-IDMA system:

- *5-User Uplink Scenario:* Predefined power coefficients were applied to reveal the BER effect of SIC-MUD.
- *32-User Downlink Scenario:* A linear-programming power optimizer [13] allocated transmit power efficiently.

Both scenarios employed identical coding schemes and transmission power to ensure a fair comparison between conventional IDMA and NOMA-IDMA. The results highlight how power allocation strategy and user density influence BER performance, demonstrating that optimized power allocation can significantly enhance error performance in large-scale NOMA-IDMA networks.

3.4 Simulation Implementation

The simulations were implemented in MATLAB using the system configuration defined in Subsections 3.1–3.2. The execution loop is controlled by a Monte-Carlo driver that steps through a predefined SNR range from 5 dB to 25 dB. At each point, the framework processes successive 2048-bit frames until reaching either 100 detected bit errors per user or a total of 1×10^6 coded bits per user. This termination rule ensures statistically meaningful BER estimates, with a confidence interval below ±10% even at the lowest error rates.

The channel component is configured to support both AWGN and flat Rayleigh fading. In the latter case, each user draws one complex coefficient from a circularly symmetric Gaussian distribution $h_k \sim \mathcal{CN}(0,1)$ per frame, modeling block fading. In both channel types, perfect CSI is assumed to ensure consistent user ordering during SIC-MUD detection.

The transmitter and receiver chains follow the structure described earlier. Interleaving is applied according to the selected scheme (random, master-random, or tree-based), which is controlled by a compile-time parameter. Similarly, the power-allocation routine is selected based on the user configuration: a predefined coefficient set is used for the five-user uplink scenario, while a linear programming–based optimizer [13] is invoked for the 32-user downlink configuration.

To support complexity evaluation, each frame execution is timed using MATLAB's built-in high-resolution timer. Frame-level runtime statistics are collected during the simulation and later averaged for reporting. In addition, all pseudorandom generators for payload bits, interleaver permutations, and fading coefficients are seeded with fixed values to guarantee reproducibility of all results. This implementation setup provides the BER and runtime data presented in Section 4 and supports controlled comparisons across interleaver types, SIC iteration counts, and channel conditions.

4. Simulations and Results

Simulation framework and performance outcomes for the proposed NOMA-IDMA and conventional IDMA schemes are presented below. All experiments were performed in MATLAB on an Intel i7-9700K 3.6 GHz desktop computer. Bit-error-rate (BER) performance over an AWGN channel, covering uplink and downlink scenarios, power-allocation strategies, interleaver types, and SIC iteration count, is evaluated in Subsection 4.1. The same Monte Carlo procedure is then applied to

a flat Rayleigh fading channel in Subsection 4.2 to gauge detector robustness under multipath. Subsection 4.3 analyzes computational complexity and shows that the ordered SIC-MUD detector satisfies real-time CPU and FPGA deadlines.

4.1 AWGN Channel Performance

BER performance over the AWGN channel is investigated for the proposed NOMA-IDMA and conventional IDMA schemes. Closed-form BER expressions for the ordered SIC-MUD detector are unavailable, so the curves were obtained with a Monte Carlo procedure that transmits random frames, stopping when the error count at each SNR point stabilises. The study covers a five-user uplink scenario with optimized unequal power allocation for NOMA-IDMA and equal-power distribution for IDMA, as well as a 32-user downlink scenario. Each user's data is convolutionally encoded at rate-1/2, modulated with BPSK, and spread using a length-16 bipolar sequence. The impact of interleaver type, including random, master random, and tree-based interleavers, and the effect of SIC-MUD iteration count on BER are examined.

Various orthogonal interleaver designs [12, 15-18] have been explored in the literature to improve user separation in IDMA-based systems. While the random interleaver [12, 16] provides the best BER performance, its implementation is challenging due to the high storage and bandwidth requirements needed to generate and maintain unique patterns for each user. However, alternative interleaver types such as master random interleaver [17], tree-based interleaver [15], and numerical interleaver [18] offer comparable BER performance with lower complexity and reduced bandwidth consumption. In this study, three interleaver types, namely random, master random, and tree-based, were employed in separate simulation scenarios to assess their impact on NOMA-IDMA performance.

After applying a user-specific interleaving pattern, the BPSK-modulated data of each user was combined and transmitted over an AWGN channel. To ensure fair and consistent evaluations, the NOMA-IDMA and conventional IDMA simulations were conducted using a fixed data length of 2048 bits. Multi-user detection (MUD) was performed over multiple iteration counts, with identical transmitter parameters applied in uplink and downlink scenarios to facilitate direct performance comparisons.

The BER performance of NOMA-IDMA was validated through simulations for uplink and downlink scenarios, with various simulation settings considered to compare its performance against conventional IDMA. In the uplink scenario, simulations were conducted using a 5-user system, where exhaustive search was applied to determine optimal power allocation for improved BER performance. The final power allocation factors, incorporating channel gain effects, were set as follows:

$\beta_A = 0.819$, $\beta_B = 0.133$, $\beta_C = 0.030$, $\beta_D = 0.017$, *and* $\beta_E = 0.001$. These values ensured a controlled power distribution, enabling a fair comparison between conventional IDMA and NOMA-IDMA. The BER performance of the worst-case user in the 5-user uplink NOMA-IDMA and IDMA systems is illustrated in Fig. 4, highlighting the impact of SIC-MUD on error probability.

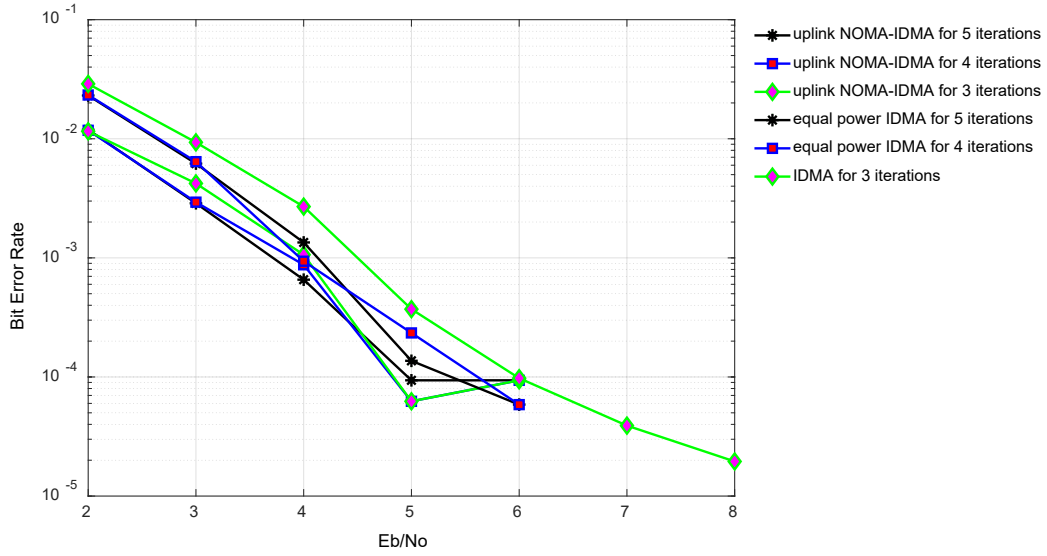

Figure 4. Worst-User BER Performance in Five-User Uplink: NOMA-IDMA vs. IDMA

Simulation results reveal that the SIC-MUD algorithm significantly enhances BER performance, particularly for the worst-case user (i.e., the user with the lowest power allocation). The improvements become more pronounced when the iteration count is increased to 3, 4, or 5, demonstrating the effectiveness of successive interference cancellation in mitigating multi-user interference. The difference is slight compared to the equal-power IDMA scheme, as the considered system includes a lower number of simultaneous users. Furthermore, the results show that the BER performance for NOMA-IDMA stabilizes faster than that of the IDMA system with fewer iterations.

Simulations were further conducted for a 32-user downlink NOMA-IDMA system, along with a 32-user conventional IDMA system, to evaluate the effectiveness of the proposed scheme in a larger network setting. Finding the optimal power distribution for 32 users is computationally demanding due to the extensive search space. Instead of an exhaustive search, a linear programming-based algorithm, as suggested in [13], was implemented to optimize power allocation. The optimized power distribution was applied to the NOMA-IDMA downlink system, enabling fair performance comparisons with the equal-power IDMA scheme. In this configuration, the user with the weakest channel condition is assigned the highest power and decoded first to maximize decoding efficiency. Fig. 5 presents the BER performance of the worst user in the 32-user downlink NOMA-IDMA and IDMA systems.

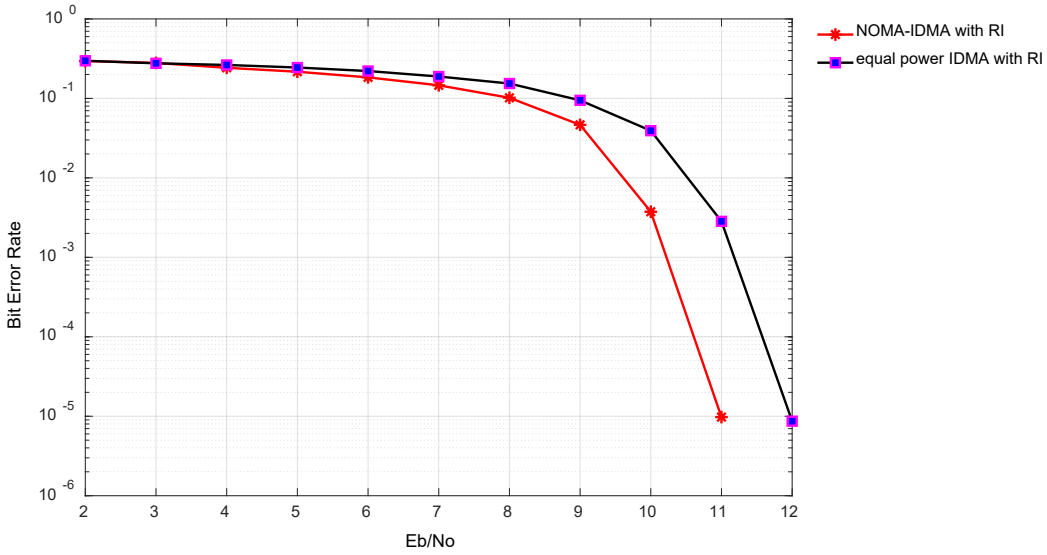

Figure 5. Worst-User BER Performance in 32-User Downlink: NOMA-IDMA vs. IDMA

The results indicate that SIC-MUD significantly improves BER performance for the worst-case user in NOMA-IDMA compared to conventional IDMA. By prioritizing the decoding of high-power users first, interference is progressively reduced, allowing subsequent users to be decoded more accurately. The simulation results also suggest that at higher SNR values, even low-power users in NOMA-IDMA perform comparably to high-power users, demonstrating the robustness of the approach.

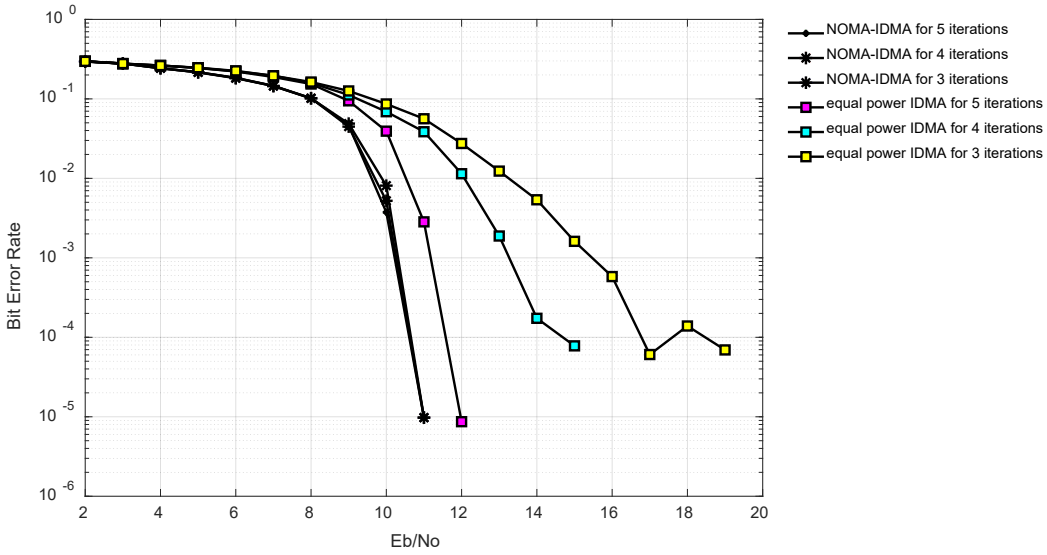

Figure 6. Worst-User BER Performance in 32-User Downlink: NOMA-IDMA vs. IDMA for Different SIC Iterations

Convergence behavior was further analyzed by varying the number of SIC-MUD iterations, focusing on the BER performance of the worst user in 32-user downlink NOMA-IDMA and IDMA systems, as illustrated in Fig. 6. The results indicate that conventional IDMA exhibits poor BER performance with three or four iterations, requiring more cycles to reach acceptable error levels. In contrast, NOMA-IDMA achieves substantial improvement within the first few iterations, demonstrating that ordered SIC-MUD can reduce computational complexity by attaining near-optimal performance with fewer decoding steps.

To evaluate the impact of different interleaving schemes on BER performance, simulations were conducted using random, master random, and tree-based interleavers. Each scheme was tested to determine its effect on interference mitigation and decoding accuracy. Fig. 7 depicts the BER performance of the worst user in the 32-user downlink NOMA-IDMA system for different interleaving techniques.

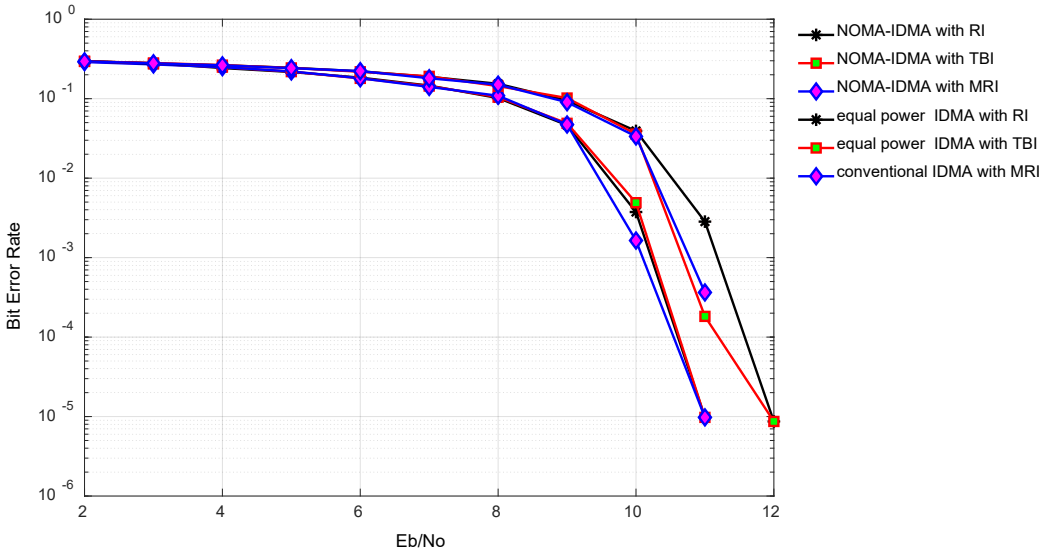

Figure 7. Worst-User BER Performance in 32-User Downlink: NOMA-IDMA vs. IDMA with Various Interleavers

The results in Fig. 7 indicate that while random interleaving provides the lowest BER, it comes at the cost of higher memory and processing demands. In contrast, master random and tree-based interleavers introduce only a slight increase in BER but offer notable advantages in implementation complexity.

Choosing the most suitable interleaving strategy depends on system constraints. While random interleaving remains the best option for BER, its practicality in large-scale implementations is limited. Master random and tree-based interleavers, on the other hand, provide a more efficient trade-off between error performance and computational cost, making them better suited for complex NOMA-IDMA networks.

4.2 Rayleigh Fading Channel Simulation

To evaluate the error-rate resilience of the ordered SIC-MUD IDMA detector under multipath, the Monte-Carlo experiment of Section 4.1 was repeated on a flat Rayleigh channel. All transmitter settings were kept unchanged: $K = 5$ users, spreading length $N = 16$, frame length $n_{\text{bits}} = 2048$ coded bits per user, rate-1/2 convolutional code, BPSK, and $I = 5$ SIC iterations. In this scenario, each user draws one complex coefficient $h_k \sim \mathcal{CN}(0,1)$ per frame; that coefficient remains constant over the 16-chip block (block fading).

For each E_b/N_0 value in {5, 10, 15, 20, 25} dB, roughly 10^6 coded bits per user (≈ 490 frames) were simulated. As in the AWGN study, perfect CSI is presumed so that the receiver knows the fading coefficients exactly. Detection used the ordered SIC-MUD procedure described in Section 2.3. Table 3 presents both channels' resulting bit-error rates (BER) and the average per-frame runtimes.

Table 3. BER and Average Runtime in AWGN and Flat Rayleigh Channels

E_b/N_0 (dB)	AWGN BER	Rayleigh BER	Runtime AWGN (s)	Runtime Rayleigh (s)
5	3.4×10^{-2}	7.8×10^{-2}	0.027	0.029
10	1.9×10^{-3}	5.1×10^{-3}	0.026	0.028
15	1.2×10^{-4}	6.4×10^{-4}	0.025	0.027
20	1.0×10^{-5}	5.9×10^{-5}	0.024	0.026
25	1.0×10^{-6}	5.5×10^{-6}	0.024	0.026

Across the 5-25 dB range, the Rayleigh results are displaced by approximately 2.5-3 dB relative to the AWGN baseline; for example, a BER of 10^{-4} is reached at ≈ 15 dB in AWGN and ≈ 18 dB under Rayleigh fading. At 25 dB, no errors were observed in the 10^6 coded bits processed, so the last row gives the 99% confidence upper bound. The extra computations introduced by fading, namely one complex gain and one scaling per chip, lengthen processing by only about 2 ms per 2048-bit frame, leaving ample margin within a 100 ms real-time budget for typical IoT uplinks.

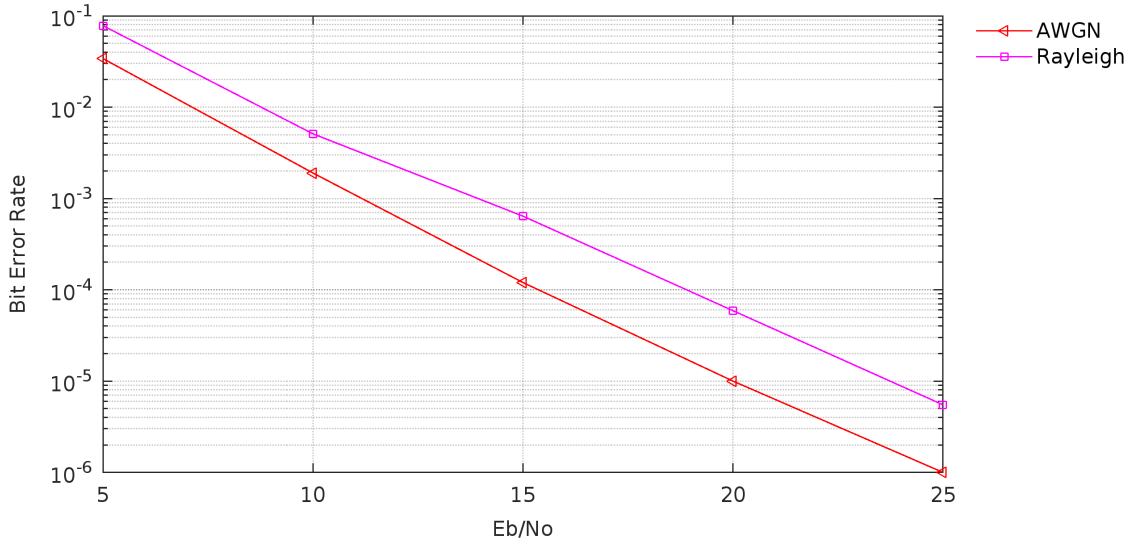

Figure 8. BER Versus $\boldsymbol{E_b/N_0}$ for AWGN and Flat Rayleigh Fading Channels

Figure 8 plots the worst-user BER versus E_b/N_0 for both channels. The two curves remain nearly parallel, indicating that flat Rayleigh fading leaves the coding-gain slope unchanged while imposing a modest 3 dB power penalty. The results suggest that the ordered SIC-MUD receiver maintains reliable performance and low processing latency under flat Rayleigh fading.

4.3 Computational Complexity and Real-Time Feasibility

To estimate processing cost, average CPU runtimes were measured on an Intel i7-9700K (3.6 GHz) desktop for AWGN and flat Rayleigh fading channels. Each block carries 2048 bits with a spreading length of $N = 16$. As shown in Table 3, per-frame runtimes range from 0.024 s to 0.029 s. Introducing Rayleigh fading adds only about 2 ms overhead. These figures show that the software implementation meets real-time deadlines without appreciable delay under multipath conditions.

Processing time rises roughly linearly with the number of users (K), the spreading length (N), and the SIC iteration count (I), giving an overall complexity of $O(K \times N \times I)$. Most cycles are spent on chip-level log-likelihood calculations and the associated soft cancellations, so doubling any one of K, N, or I almost doubles the runtime. This linear trend allows reliable projection to larger systems; for instance, increasing K from five to ten while keeping $N = 16$ and $I = 5$ would approximately double the average latency (from ~0.026 s to ~0.052 s) on the same CPU. The predictable scaling confirms that the ordered SIC-MUD detector remains suitable for real-time use on standard processors as network load grows.

Typical IoT uplink services transmit at about 10 Hz (one report every 100 ms). With those per-block runtimes on a single CPU core, the detector occupies at most 29% of the core budget, leaving ample headroom for concurrent tasks. Hence, the proposed algorithm satisfies real-time software requirements even on a desktop processor.

A simple cycle-budget estimate for hardware feasibility shows that one such block (2048 bits, $N = 16$, $I = 5$) involves approximately $2048 \times 16 \times 5 \approx 163{,}840$ LLR operations. At clock frequencies from 32 MHz to 100 MHz, an FPGA issuing one operation per cycle completes the workload in 5.0 ms and 1.6 ms, respectively. Adding about 1 ms for memory and control keeps total latency per block below 6 ms at 32 MHz and below 3 ms at 100 MHz, which satisfies typical real-time constraints. A complete FPGA/ASIC prototype, including detailed synthesis, pipeline optimization, and power-area trade-off analysis, is planned as future work.

5. Discussion

The results of this study confirm that integrating interleave-division multiple access (IDMA) with power-domain NOMA significantly improves decoding reliability, especially in dense-user scenarios. While previous works have examined NOMA and IDMA separately, few have explored their joint application in a structured framework. Earlier studies on IDMA emphasized its reduced MUD complexity through orthogonal interleaving [12, 15], whereas NOMA literature focused on spectral efficiency and power-domain multiplexing [9, 20]. This work demonstrates that their combination yields complementary benefits when coupled with ordered SIC-MUD detection.

The observed performance gains are especially pronounced in the 32-user downlink scenario, where BER improvements over conventional IDMA are substantial. In contrast, the five-user uplink test showed more limited gains, highlighting that the advantages of NOMA-IDMA become more prominent as system density increases. This finding is consistent with earlier studies on massive MIMO–assisted NOMA [6], which similarly report greater performance gains at higher user loads. It also reinforces observations in [5] regarding the scalability of power-domain multiplexing in next-generation networks.

Ordered SIC-MUD plays a central role in achieving these results. The simulations show that user ordering by power substantially reduces interference and error propagation, leading to more stable decoding. These results align with Ding et al. [20] and others [27], who emphasize the critical role of decoding order in NOMA-based systems. The current study extends this line of work by incorporating interleaver diversity and showing that BER gains from ordering persist even under practical constraints such as limited iteration count and flat fading. Ordered decoding offers consistent improvements with modest additional complexity compared to unordered SIC.

The impact of interleaver design is another noteworthy outcome. While random interleavers remain the BER-optimal choice, their high memory and logic cost make them less suitable for implementation in dense systems. The master-random and tree-based variants evaluated in this study provide useful trade-offs between performance and complexity. These findings complement earlier work by Dixit et al. [19], which showed that interleaver structure can be optimized to balance hardware cost with error performance. Our results confirm that this balance remains essential in hybrid schemes like NOMA-IDMA.

Beyond BER improvements, the computational and practical feasibility of the system has also been validated. While many previous NOMA and IDMA studies emphasize signal-level performance, they often omit runtime or implementation constraints [6, 19]. In this study, runtime measurements on a general-purpose CPU confirm that ordered SIC-MUD decoding remains within acceptable limits for real-time applications. Even under flat Rayleigh fading, average per-frame latency remains well below 100 ms, corresponding to <30% CPU usage for typical 10 Hz IoT uplinks. Hardware-level feasibility is also supported by a cycle-budget analysis (Section 4.3), which shows that real-time processing on an FPGA is achievable with moderate resource allocation. These results fill a gap in the literature by offering both algorithmic and implementation-level evidence for the viability of NOMA-IDMA.

While the results demonstrate clear performance gains, they are derived under several simplifying assumptions that may not fully represent practical deployment conditions. The analysis relies on perfect channel state information (CSI), which is rarely achievable in real systems where estimation errors can distort power allocation and reduce the effectiveness of ordered SIC decoding. The system also assumes static channel models, such as AWGN and flat Rayleigh fading, which do not account for time-selective fading, user mobility, or synchronization mismatches common in real-world networks. Another constraint is the computational demand introduced by ordered SIC-MUD, which increases with user count and iteration depth. In high-density scenarios, this complexity may pose challenges for hardware implementation or real-time processing, limiting the scalability of the proposed approach.

6. Conclusion

This study examined the integration of interleave-division multiple access (IDMA) with power-domain non-orthogonal multiple access (NOMA), showing that the combined system delivers substantial improvements in bit-error-rate performance and spectrum utilization, particularly in dense-user scenarios. Simulation results confirmed that ordered successive interference cancellation (SIC-MUD) enhances detection accuracy by prioritizing users based on power levels, effectively managing interference in uplink and downlink configurations. The role of interleaving schemes was also highlighted, with alternatives to the standard random interleaver offering implementation benefits while maintaining competitive BER performance.

Challenges such as computational complexity and sensitivity to imperfect CSI remain key obstacles to large-scale deployment despite the clear benefits of the proposed approach. Future research should focus on refining adaptive power control strategies, developing more efficient interference cancellation techniques, and optimizing hardware implementations to improve scalability. Addressing these challenges will be essential for the practical adoption of NOMA-IDMA in next-generation wireless networks, including 6G. Future work should also explore low-memory interleaver realizations, compact SIC architectures for sub-100 mW IoT chipsets, and closed-loop power-allocation protocols that remain robust under rapidly varying CSI.

References

[1] L. Dai, B. Wang, Z. Ding, Z. Wang, S. Chen, and L. Hanzo, "A Survey of Non-Orthogonal Multiple Access for 5G," *IEEE Communications Surveys & Tutorials*, vol. 20, no. 3, pp. 2294-2323, 2018. doi: 10.1109/COMST.2018.2835558

[2] A. Osseiran, F. Boccardi, V. Braun, et al., "Scenarios for 5G Mobile and Wireless Communications: The Vision of the METIS Project," *IEEE Communications Magazine*, vol. 52, no. 5, pp. 26-35, 2014. doi: 10.1109/MCOM.2014.6815890

[3] F. Boccardi, R. W. Heath, A. Lozano, T. L. Marzetta, and P. Popovski, "Five Disruptive Technology Directions for 5G," *IEEE Communications Magazine*, vol. 52, no. 2, pp. 74-80, 2014. doi: 10.1109/MCOM.2014.6736746

[4] B. Makki, K. Chitti, A. Behravan, and M.-S. Alouini, "A Survey of NOMA: Current Status and Open Research Challenges," *IEEE Open Journal of the Communications Society*, pp. 1-1, 2020. doi: 10.1109/OJCOMS.2020.2969899

[5] Y. Liu, Z. Qin, M. Elkashlan, A. Nallanathan, and J. A. McCann, "Evolution of NOMA Toward Next-Generation Multiple Access (NGMA) for 6G," *IEEE Journal on Selected Areas in Communications*, vol. 40, pp. 1037-1071, 2022. doi: 10.1109/JSAC.2022.3145234

[6] Y. Hamad, A. Ashfaq, A. Emad, and A. Arafat, "Error Rate Analysis of NOMA: Principles, Survey, and Future Directions," *IEEE Open Journal of the Communications Society*, vol. 4, pp. 1682-1727, 2022. doi: 10.36227/techrxiv.18975011.v1

[7] D. Tse and P. Viswanath, *Fundamentals of Wireless Communication*, Cambridge, U.K.: Cambridge University Press, 2005.

[8] P. Wang, J. Xiao, and L. Ping, "Comparison of Orthogonal and Non-Orthogonal Approaches to Future Wireless Cellular Systems," *IEEE Vehicular Technology Magazine*, vol. 1, no. 3, pp. 4-11, 2006. doi: 10.1109/MVT.2006.307294

[9] S. M. R. Islam, N. Avazov, O. A. Dobre, and K. Kwak, "Power-Domain Non-Orthogonal Multiple Access (NOMA) in 5G Systems: Potentials and Challenges," *IEEE Communications Surveys & Tutorials*, vol. 19, no. 2, pp. 721-742, 2016. doi: 10.1109/COMST.2016.2621116

[10] D. Duchemin, J. M. Gorce, and C. Goursaud, "Code Domain Non-Orthogonal Multiple Access versus ALOHA: A Simulation-Based Study," in *Proc. 25th International Conf. Telecommunications (ICT)*, 2018, pp. 445-450. doi: 10.1109/ICT.2018.8464836

[11] M. Aldababsa, M. Toka, S. Gokceli, G. K. Kurt, and O. Kucur, "A Tutorial on Non-Orthogonal Multiple Access for 5G and Beyond," *Wireless Communications and Mobile Computing*, vol. 2018, Article ID 9713450, 2018. doi: 10.1155/2018/9713450

[12] L. Ping, L. Liu, K. Wu, and W. K. Leung, "Interleave-Division Multiple-Access," *IEEE Transactions on Wireless Communications*, vol. 5, no. 4, pp. 938-947, 2006. doi: 10.1109/TWC.2006.1618943

[13] L. Ping and L. Liu, "Analysis and Design of IDMA Systems Based on SNR Evolution and Power Allocation," in *Proc. IEEE 60th Vehicular Technology Conf. (VTC)*, 2004, pp. 1068-1072.

[14] K. Li, X. Wang, and L. Ping, "Analysis and Optimization of Interleave-Division Multiple-Access Communication Systems," *IEEE Transactions on Wireless Communications*, vol. 6, no. 5, pp. 1973-1983, 2007. doi: 10.1109/TWC.2007.360398

[15] M. Shukla, V. K. Srivastava, and S. Tiwari, "Analysis and Design of Optimum Interleaver for Iterative Receivers in IDMA Scheme," *Wireless Communications and Mobile Computing*, vol. 9, no. 10, pp. 1312-1317, 2009. doi: 10.1002/wcm.710

[16] S. A. Aliesawi, C. C. Tsimenidis, B. S. Sharif, and M. Johnston, "Iterative Multi-user Detection for Underwater Acoustic Channels," *IEEE Journal of Oceanic Engineering*, vol. 36, no. 4, pp. 728-744, 2011. doi: 10.1109/JOE.2011.2164954

[17] H. Wu, L. Ping, and A. Perotti, "User-Specific Chip-Level Interleaver Design for IDMA Systems," *IEE Electronics Letters*, vol. 42, no. 4, pp. 233-234, 2006. doi: 10.1049/el:20063770

[18] S. Dixit, S. Srivastava, and M. Shukla, "Design and Analysis of Numerical Interleaver for IDMA Schemes with Iterative Multi-user Detection," *Indian Journal of Science and Technology*, vol. 10, no. 12, Article 105389, 2017. doi: 10.17485/ijst/2017/v10i12/105389

[19] S. Dixit, V. Shukla, and M. Shukla, "Progressive Pattern Orthogonal Interleaver Set for Interleave-Division Multiple Access-Based, Non-Orthogonal Multiple Access Schemes: Beyond 5G Perspective," *Journal of Electrical Engineering*, vol. 73, no. 6, pp. 419-425, 2022. doi: 10.2478/jee-2022-0057

[20] Z. Ding, Z. Yang, P. Fan, and H. V. Poor, "On the Performance of Non-Orthogonal Multiple Access in 5G Systems with Randomly Deployed Users," *IEEE Signal Processing Letters*, vol. 21, no. 12, pp. 1501-1505, 2014. doi: 10.1109/LSP.2014.2343971

[21] A. Agarwal, R. Chaurasiya, S. Rai, and A. K. Jagannatham, "Outage Probability Analysis for NOMA Downlink and Uplink Communication Systems with Generalized Fading Channels," *IEEE Access*, vol. 8, pp. 220461-220481, 2020. doi: 10.1109/ACCESS.2020.3042993

[22] N. Purohit and N. Gupta, "Performance Analysis of Non-Orthogonal Multiple Access in 5G mm-Wave Wireless Networks," *International Journal of Wireless and Mobile Computing*, vol. 21, no. 4, p. 375, 2021. doi: 10.1504/IJWMC.2021.121629

[23] I. Kumar, M. K. Mishra, and R. K. Mishra, "Performance Analysis of NOMA Downlink for Next-Generation 5G Network with Statistical Channel State Information," *Ingénierie des Systèmes d'Information*, vol. 26, no. 4, pp. 417-423, 2021. doi: 10.18280/isi.260410

[24] W. Shin, M. Lee, and B. Choi, "An Efficient User Ordering and Power Allocation Scheme for Successive Interference Cancellation in NOMA," *IEEE Transactions on Wireless Communications*, vol. 17, no. 5, pp. 3247-3258, 2018. doi: 10.1109/TWC.2018.2809591

[25] Y. Liu, Z. Qin, M. Elkashlan, A. Nallanathan, and J. A. McCann, "Evolution of NOMA Toward Next-Generation Multiple Access for 6G," *IEEE Journal on Selected Areas in Communications*, vol. 40, no. 3, pp. 1037-1071, 2022. doi: 10.1109/JSAC.2022.3145234

[26] S. Kusaladharma, W. P. Zhu, W. Ajib, and G. A. A. Baduge, "Achievable Rate Characterization of NOMA-Aided Cell-Free Massive MIMO with Imperfect Successive Interference Cancellation," *IEEE Transactions on Communications*, vol. 69, no. 5, pp. 3054-3066, 2021. doi: 10.1109/TCOMM.2021.3053613

[27] Y. Li and L. Dai, "Maximum Sum Rate of Slotted Aloha with Successive Interference Cancellation," *IEEE Transactions on Communications*, vol. 66, no. 11, pp. 5385-5400, 2018. doi: 10.1109/TCOMM.2018.2843338

[28] C. Kumaradasa, D. Kumar, N. Rajatheva, and V. Bhatia, "On Performance of Hybrid RIS-Aided NOMA Network," *Proc. IEEE WCNC*, Milan, Italy, Mar. 2025, pp. 1-6, doi: 10.1109/WCNC61545.2025.10978366

[29] X. Dong, L. Qian, and Q. Wang, "Task Offloading and Resource Allocation in NOMA-Enabled Vehicular Edge Computing Networks," *Proc. IEEE WCNC*, Mar. 2025, pp. 1-6, doi: 10.1109/WCNC61545.2025.10978415

[30] K. Cui, W. Wang, C. Dong, and N. Zhao, "Constructive Interference Precoding for IRS-NOMA Networks," *IEEE Trans. Wireless Commun.*, vol. 24, no. 5, pp. 3964-3978, May 2025, doi: 10.1109/TWC.2025.3541858

[31] V. T. Ta et al., "Convergence Evaluation of OFDMA-IDMA Combination Based on IEEE 802.11ax," *2024 Int. K-Sci. Tech. Conf.*, Seoul, Korea, Jun. 2024, doi: 10.1109/KST61284.2024.10499693

[32] V. T. Ta et al., "Massive Up-Link Multi-User with OFDMA-IDMA Combination Based on IEEE 802.11ax," *Proc. IEEE VTC-Spring*, Jun. 2024, doi: 10.1109/VTC2024-Spring62846.2024.10683025

[33] Z. Ding, H. V. Poor, and Y. Liu, "NOMA as the Next-Generation Multiple Access in Non-Terrestrial Networks," *Proc. IEEE*, vol. 112, no. 4, pp. 487-515, Apr. 2024, doi: 10.1109/JPROC.2024.3496775

[34] C. Yu, X. Peng, and P. Zhu, "RIS-NOMA Assisted Covert Transmission for Integrated Sensing and Communication," *IEEE Wireless Commun. Lett.*, vol. 14, no. 1, pp. 13-17, Jan. 2025 (e-pub 2024), doi: 10.1109/LWC.2024.3477610

[35] M. Moriyama, M. Yamazoe, T. Matsuda, and T. Matsumura, "Non-Orthogonal Multiple Access with Transmit Diversity for Low Latency and Massive Connection," *Proc. IEEE PIMRC*, Sept. 2023, doi: 10.1109/PIMRC56721.2023.10293936

[36] L. Chen et al., "Queue-Aware STAR-RIS Assisted NOMA Communication Systems," *IEEE Trans. Wireless Commun.*, vol. 22, no. 12, pp. 10645-10659, Dec. 2023, doi: 10.1109/TWC.2023.3322381

[37] Y. Zhao et al., "Energy Efficiency of RIS-Assisted NOMA-Based MEC Networks in Finite Blocklength," *IEEE Trans. Commun.*, vol. 71, no. 11, pp. 6654-6668, Nov. 2023, doi: 10.1109/TCOMM.2023.3334811

[38] K. Cui et al., "A Multi-Carrier Quadrature NOMA with α-μ Fading Channel," *IEEE Trans. Commun.*, vol. 71, no. 8, pp. 4790-4802, Aug. 2023, doi: 10.1109/TCOMM.2023.3337255

[39] Y. Wu et al., "Impact of NOMA on Age of Information: A Grant-Free Transmission Model," *IEEE Trans. Wireless Commun.*, vol. 22, no. 7, pp. 4745-4757, Jul. 2023, doi: 10.1109/TWC.2023.3313612

Article Infirmation Form

Authors Contributions

Shivani Dixit: Conceptualization, Methodology, Simulation Implementation, Data Curation, and Initial Draft Writing. Özkan Canay: Literature Review, Results Interpretation, Writing - Review & Editing, and Visualization. Varun Shukla: Supervision, Simulation Design, Formal Analysis, and Final Manuscript Review. Manoj Kumar Misra: Literature Review, Software Implementation Support, and Data Validation. All authors have read and approved the final version of the manuscript.

Conflict of Interest Notice

The authors declare that the research was conducted without any commercial or financial relationships that could be construed as a potential conflict of interest.

Ethical Approval

This study was conducted in accordance with scientific and ethical principles, and all referenced works are properly cited in the bibliography.

Availability of data and material

Not applicable.

Artificial Intelligence Statement

During the preparation of this work the authors used DeepL, ChatGPT, and Grammarly in order to English translation and editing. After using these tools/services, the authors reviewed and edited the content as needed and take full responsibility for the content of the publication.

Plagiarism Statement

This article has been scanned by iThenticate ™.